Hindawi Publishing Corporation
International Journal of Antennas and Propagation
Volume 2012, Article ID 538161, 9 pages
doi:10.1155/2012/538161

Research Article

Impact of Antenna Placement on Frequency Domain Adaptive Antenna Array in Hybrid FRF Cellular System

Sri Maldia Hari Asti, Wei Peng, and Fumiyuki Adachi

Department of Communication Engineering, Graduate School of Engineering, Tohoku University, 6-6-05 Aza-Aoba, Aramaki, Aoba-ku, Sendai 980-8579, Japan

Correspondence should be addressed to Wei Peng, peng@mobile.ecei.tohoku.ac.jp

Received 6 July 2012; Accepted 7 September 2012

Academic Editor: Guangyi Liu

Frequency domain adaptive antenna array (FDAAA) is an effective method to suppress interference caused by frequency selective fading and multiple-access interference (MAI) in single-carrier (SC) transmission. However, the performance of FDAAA receiver will be affected by the antenna placement parameters such as antenna separation and spread of angle of arrival (AOA). On the other hand, hybrid frequency reuse can be adopted in cellular system to improve the cellular capacity. However, optimal frequency reuse factor (FRF) depends on the channel propagation and transceiver scheme as well. In this paper, we analyze the impact of antenna separation and AOA spread on FDAAA receiver and optimize the cellular capacity by using hybrid FRF.

1. Introduction

Single-carrier (SC) transmission has been adopted for uplink transmission in LTE [1] and LTE-A [2] systems due to its wide coverage and lower peak-to-average power ratio (PAPR) than multicarrier (MC) transmission. However, the wireless channel becomes severely frequency selective as the data rate increases due to the multiple paths with different time delays [3]. In such a frequency-selective channel, interblock interference (IBI) and intersymbol interference (ISI) are produced and degrade the transmission significantly. To deal with this problem, cyclic prefix (CP) will be inserted at the transmitter side, and then be removed at the receiver side to avoid IBI and frequency domain equalization (FDE) technique has been proposed to suppress ISI in SC transmission [3]. FDE equalizes the frequency domain receive signal by applying equalization weight to combat the channel fluctuation in each frequency. Several methods to calculate FDE weight have been introduced, such as zero-forcing (ZF), minimum-mean-square error (MMSE), and so forth.

In cellular system, neighboring cells will use the same carrier frequency/frequencies to save the bandwidth and cochannel interference (CCI) exists and CCI power will be determined by the distance between cochannel cells. In addition, the existence of multiple users within the same cell will cause multiuser interference (MUI). As a result, cellular capacity will be limited by multiple access interference (MAI, which includes both CCI and MUI) instead of additive noise. Adaptive antenna array (AAA) is a powerful method to combat MAI. It has been proved in [4] that AAA receiver can effectively deal with up to $N_r - 1$ interferences when flat fading channel is assumed where N_r represents the number of antenna elements in the array.

Therefore, in order to combat the MAI in frequency selective fading channel, it is natural for us to resort to both FDE and AAA. In our previous study [5], frequency domain adaptive antenna array (FDAAA) has been proposed and proved to be more effective to suppress MUI in severe frequency selective fading channel than the other frequency domain algorithms such as diversity combing algorithm. However, the performance of antenna array will depend

on antenna placement, which determines the coupling and radiation pattern between antennas. In addition, the angle of arrival (AOA) of the receive signals' waveform will also affect the performance [6, 7]. These considerations have not been addressed in our previous study and, to the best of our knowledge, have not been addressed in the literature.

On the other hand, cellular capacity is determined by the bandwidth efficiency and the available bandwidth. By increasing the frequency reuse factor (FRF), the distance between cochannel cells will increase, and the CCI power will be reduced. However, the available bandwidth is reduced at the same time. As a result, cellular capacity becomes a tradeoff between bandwidth efficiency and available bandwidth, which is determined by FRF. In our previous study [8], hybrid FRF has been proposed to optimize the cellular capacity. However, the optimal FRF depends on the channel propagation model and transceiver structure. And the cellular capacity optimization problem has to be reformulated when FDAAA receiver is considered.

In this paper, we optimize the cellular capacity in SC uplink transmission using FDAAA receiver by taking into consideration the impact of antenna placement. The remaining of the paper is organized as follows: uplink FDAAA receiver for cellular system is introduced in Section 2; Hybrid FRF algorithm and analysis on cellular capacity is given in Section 3; In Section 4, the impact of antenna placement, that is, antenna separation and AOA spread, will be analyzed; Numerical results on cellular capacity will then be given in Section 5 and finally the paper will be concluded in Section 6.

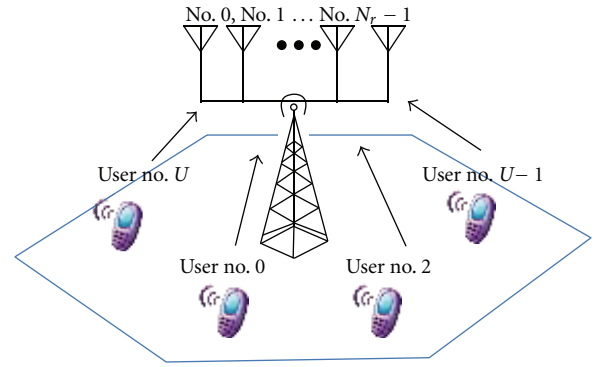

Figure 1: Uplink transmission in a single cell.

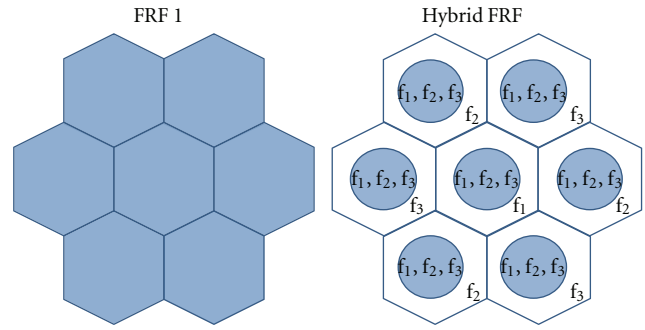

Figure 2: Structure of single FRF and hybrid FRF.

2. Uplink FDAAA Receiver in Cellular System

2.1. System Model. It is assumed that the base station (BS) locating at the center of each cell is equipped with N_r antennas, and there are U mobile stations (MSs, that is, users) in each cell and each user is equipped with a single transmit antenna, as shown in Figure 1. We assume that the *0*th user is the desired user, and the other users are interfering users, it is also assumed that the channel remains unchanged during one block transmission. Two cellular structures are shown in Figure 2. On the left is the conventional cellular structure using single FRF (FRF 1), on the right is the cellular structure using hybrid FRF which will be further explained in Section 3.

The channel impulse response between the uth user and the BS can be expressed as

$$\mathbf{h}_u(\tau) = \sum_{l=0}^{L-1} \mathbf{h}_{u,l}\delta(\tau - \tau_l), \tag{1}$$

where $\mathbf{h}_{u,l}$ and τ_l are the channel gain vector and time delay of the lth path, respectively, $\sum_{l=0}^{L-1} E\{|h_{u,m,l}|^2\} = 1$ where $h_{u,m,l}$ is the mth element of $\mathbf{h}_{u,l}$ and $E\{\cdot\}$ denotes statistical expectation. The path delay is assumed to be integer multiples of symbol duration and $\tau_l = l$. CP is used and its length is assumed to be longer than the maximum path delay so that IBI can be avoided.

The baseband receive signal vector $\mathbf{r}(n) = [r_0(n), r_1(n), \ldots, r_{N_r-1}(n)]^T$, $(n = 1, \ldots, N_c)$ is given by

$$\begin{aligned}\mathbf{r}(n) = {} & \sqrt{P_0 {d_0}^{-\alpha} 10^{-\xi_0/10}} \sum_{l=0}^{L-1} \mathbf{h}_0 s_0(n - \tau_l) \\ & + \sum_{u=1}^{U-1} \sqrt{P_u {d_u}^{-\alpha} 10^{-\xi_u/10}} \sum_{l=0}^{L-1} \mathbf{h}_u s_u(n - \tau_l) \\ & + \sum_{i=0}^{I-1} \sum_{u=0}^{U-1} \sqrt{P_{u,i} {d_{u,i}}^{-\alpha} 10^{-\xi_{u,i}/10}} \\ & \times \sum_{l=0}^{L-1} \mathbf{h}_{u,i} s_{u,i}(n - \tau_l) + z(n),\end{aligned} \tag{2}$$

where U and I are the number of users per cell and the number of cochannel cells, respectively; Subscripts u and (u, i) represent the index of the uth user at the desired cell and at the ith cochannel cell, respectively; P represents the transmit power; s is the transmit signal; d represents the normalized distance between the user and the BS of the desired cell; α and ξ represent the path loss exponent and shadowing loss, respectively. $\mathbf{z}(n) = [z_0(n) \ \ldots \ z_{N_r-1}(n)]^T$ is the vector of complex additive white Gaussian noise (AWGN). In this study, slow transmit power control (TPC) in each cell is assumed so that each user will have the same

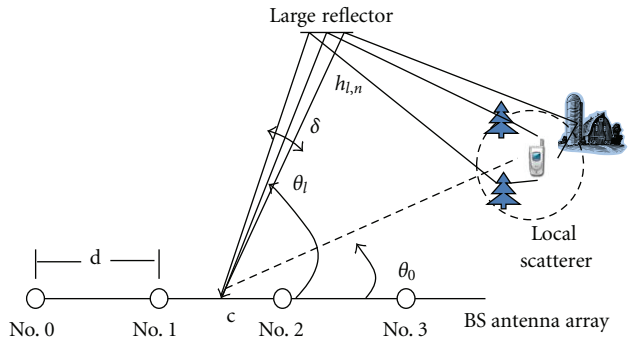

FIGURE 3: Propagation model of linear antenna array.

target receive signal power in average at the corresponding BS. Therefore, the transmit power is given by

$$P_u = \left(\frac{P_{\text{target}}}{{d_u}^{-\alpha}10^{-\xi_u/10}}\right) {d_{u,0}}^{-\alpha}10^{-\xi_{u,0}/10}, \tag{3}$$

where P_{target} is the target receive signal power; The frequency domain received signal on the kth frequency is then expressed as

$$\begin{aligned}\mathbf{R}(k) &= \mathbf{H}_0(k)S_0(k) + \sum_{u=1}^{U-1}\mathbf{H}_u(k)S_u(k) \\ &\quad + \sum_{i=0}^{I-1}\sum_{u=0}^{U-1}\mathbf{H}_{u,i}(k)S_{u,i}(k) + \mathbf{Z}(k),\end{aligned} \tag{4}$$

where $\mathbf{H}_u = [H_{u,0}(k)\ \ H_{u,1}(k)\ \ \ldots\ \ H_{u,N_r-1}(k)]^T$, $S_u(k)$, and $\mathbf{Z}(k) = [Z_0(k)\ \ Z_1(k)\ \ \ldots\ \ Z_{N_r-1}(k)]^T$ are, respectively, the frequency domain channel response, transmit signal, and noise component, given by (5). In the right hand side of (4), the first term comes from the desired user, the second term comes from MUI, the third term comes from CCI, and the last term is the noise component.

$$\begin{aligned}S_u(k) &= \sqrt{P_u {d_u}^{-\alpha}10^{-\xi_u/10}}\sum_{n=0}^{N_c-1}s_u(n)\exp\left(-j2\pi n\frac{k}{N_c}\right), \\ H_{u,m}(k) &= \sum_{l=0}^{L-1}\sum_{n=0}^{N_c-1}h_{u,l,m}\exp\left(-j2\pi n\frac{k}{N_c}\right), \\ Z_m(k) &= \sum_{n=0}^{N_c-1}z_m(n)\exp\left(-j2\pi n\frac{k}{N_c}\right).\end{aligned} \tag{5}$$

2.2. Propagation Model of Adaptive Antenna Array. Linear antenna array is assumed, and the propagation model is shown in Figure 3. The geometric center of array is denoted by c and the antenna separation is denoted by d. θ_0 represents the angle between line of sight (LOS) direction of MS and the BS array plane; The plane waveform of the lth path from the uth user is consisted of a number of unresolvable paths and the angle spread of the unresolvable paths is denoted by δ; In this study, δ is assumed to be zero for simplicity and $h_{u,l}$ represents the plane waveform of lth path from the uth user. The nominal AOA of $h_{u,l}$ observed at array center c is denoted by $\theta_{u,l}$ and the AOA spread of $\theta_{u,l}$ is uniformly distributed within a range of Δ. Therefore, the lth path gain of the uth user which is observed at the mth antenna element can be given by

$$h_{u,l,m} = h_{u,l}\exp\left(-j2\pi\frac{(0.5M - m + 0.5)}{\lambda}d\cos\theta_{u,l}\right), \tag{6}$$

where $m = 1, 2, 3, \ldots, N_r$ and λ is the carrier wavelength.

2.3. FDAAA Receiver. In our previous study, FDAAA receiver has been investigated in [5–7]. The transceiver structure of SC transmission using FDAAA receiver is shown in Figure 4. At the receiver side, the CP is removed and the receive signal at each antenna is transformed to frequency domain by using fast Fourier transform (FFT), then adaptive antenna array (AAA) weight control is then performed on each frequency and the output after AAA weight control is given by [9]:

$$\hat{R}(k) = \mathbf{W}_{\text{FDAAA}}^H(k)\mathbf{R}(k), \tag{7}$$

where $\mathbf{W}_{\text{FDAAA}}(k) = [W_{\text{FDAAA},0}(k), W_{\text{FDAAA},1}(k), \ldots, W_{\text{FDAAA},N_r-1}(k)]^T$ minimizes the mean square error (MMSE) between $\hat{R}(k)$ and the frequency domain desired signal $S_0(k)$, given by [5–7]:

$$\mathbf{W}_{\text{FDAAA}}(k) = \mathbf{X}(k)^{-1}\mathbf{p}(k), \tag{8}$$

where $\mathbf{X}(k) = E\{\mathbf{R}(k)\mathbf{R}(k)^H\}$ is the autocorrelation matrix of the received signal vector, $\mathbf{p}(k) = E\{\mathbf{R}(k){S_0}^*(k)\}$ is the cross-correlation between the receive signal and the reference signal, superscript H denotes Hermitan transposition, and $*$ denotes the complex conjugate operation. It is assumed that the transmit signals from different users are independent and the noise component is also independent to them. The autocorrelation matrix $\mathbf{X}(k)$ is an $N_r \times N_r$ square matrix, and the (m, n)th element of $\mathbf{X}(k)$ is given by

$$\begin{aligned}X_{m,n}(k) &= E\{R_m(k){R_n}^*(k)\} \\ &= E\left\{H_{0,m}(k)S_0(k)S_0^*(k)H_{0,n}^*(k)\right\} \\ &\quad + \sum_{u=1}^{U-1}E\left\{H_{u,m}(k)S_u(k)S_u^*(k)H_{u,n}^*(k)\right\} \\ &\quad + \sum_{i=0}^{I-1}\sum_{u=0}^{U-1}E\left\{H_{u,i,m}(k)S_{u,i}(k)S_{u,i}^*(k)H_{u,i,n}^*(k)\right\} \\ &\quad + E\{Z_m(k)Z_n^*(k)\}.\end{aligned} \tag{9}$$

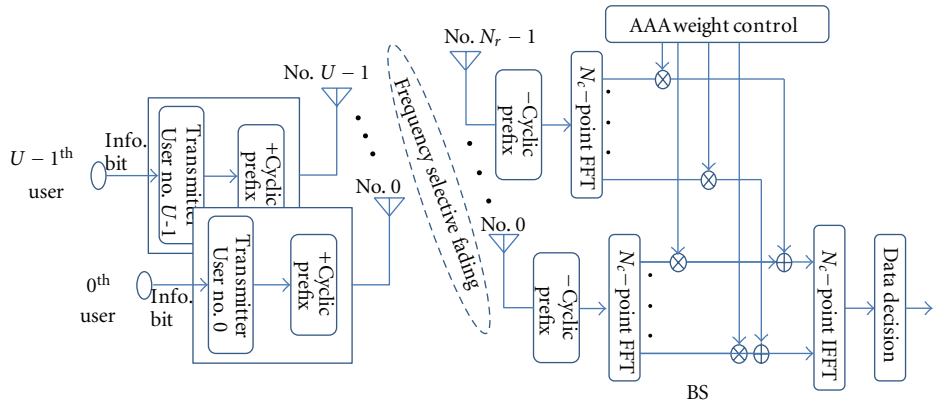

Figure 4: FDAAA uplink transmission.

Since channel state information (CSI) is known for the users within the cell of interest, (9) can be rewritten as

$$\begin{aligned} X_{m,n}(k) &= B_0 H_{0,m}(k) H_{0,n}^*(k) \\ &\quad + \sum_{u=1}^{U-1} P_{\mathrm{MUI},u} H_{u,m}(k) H_{u,n}^*(k) \\ &\quad + \sum_{i=0}^{I-1} \sum_{u=0}^{U-1} \mathrm{diag}\left[P_{\mathrm{CCI},u,i}\right]_{N_r \times N_r} \\ &\quad + \sigma^2 \mathbf{I}, \end{aligned} \tag{10}$$

where B_0 is received signal power of the desired user; $P_{\mathrm{MUI},u}$ and $P_{\mathrm{CCI},u}$ represent MUI and CCI power from the uth user, respectively. Similarly, the mth element of the cross correlation matrix can be given by

$$p_m(k) = E\{R_m(k) S_0{}^*(k)\} = B_0 H_{0,m}(k). \tag{11}$$

Data decision is then made based on the time domain signal estimate which is obtained by applying inverse FFT (IFFT) to the frequency domain signal component in (7), given by

$$\hat{r}(n) = \frac{1}{N_c} \sum_{k=0}^{N_c-1} \hat{R}(k) \exp\left(j2\pi k \frac{n}{N_c}\right). \tag{12}$$

3. Hybrid FRF Algorithm and Capacity Analysis

3.1. Hybrid FRF. Different from traditional cellular system which uses the same FRF for the whole cell, hybrid FRF algorithm adopts FRF = 1 and FRF = 3 adaptively to optimize the cellular structure [10]. According to the location and instantaneous channel status of a user, hybrid FRF algorithm uses FRF 1 for area near the cell center and FRF 3 for area near the edge cell. As a result, two data rates coexist within a cell. Since the same target receive power P_{target} is required for users with different data rates, the relation between energy and power is given as

$$\frac{E_s}{N_0} = \frac{P_{\mathrm{target}} \times T_s}{N_0}, \tag{13a}$$

$$\frac{P_{\mathrm{target}}}{N_0} = \begin{cases} \mathrm{BW} \times \left(\dfrac{E_s}{N_0}\right)_{\mathrm{target}}, & \text{cell center,} \\ \dfrac{\mathrm{BW}}{3} \times \left(\dfrac{E_s}{N_0}\right)_{\mathrm{target}}, & \text{cell edge,} \end{cases} \tag{13b}$$

where T_s is symbol period, and BW is the bandwidth. Receive power from the uth user at the desired BS and at the ith cochannel BS are given by (14) and (15), respectively.

$$\frac{B_u}{N_0} = \left(\frac{P_{\mathrm{target}}/N_0}{{d_u}^{-\alpha} 10^{-\xi_u/10}}\right) {d_u}^{-\alpha} 10^{-\xi_u/10}, \tag{14a}$$

$$B_u = \begin{cases} (E_s)_{\mathrm{target}} \times \mathrm{BW}, & \text{cell center,} \\ (E_s)_{\mathrm{target}} \times \dfrac{\mathrm{BW}}{3}, & \text{cell edge,} \end{cases} \tag{14b}$$

$$\frac{B_{u,i}}{N_0} = \left(\frac{P_{\mathrm{target}}/N_0}{{r_{u,i}}^{-\alpha} 10^{-\eta_{u,i}/10}}\right) {d_{u,i}}^{-\alpha} 10^{-\xi_{u,i}/10}, \tag{15a}$$

$$\begin{aligned} B_{u,i} &= \left(\frac{P_{\mathrm{target}}}{\hat{r}_{u,i}^{-\alpha} 10^{-\eta_{u,i}/10}}\right) {d_{u,i}}^{-\alpha} 10^{-\xi_{u,i}/10} \\ &= \begin{cases} \left(\dfrac{(E_s)_{\mathrm{target}} \times \mathrm{BW}}{{r_{u,i}}^{-\alpha} 10^{-\eta_{u,i}/10}}\right) {d_{u,i}}^{-\alpha} 10^{-\xi_{u,i}/10}, & \text{cell center,} \\ \left(\dfrac{(E_s)_{\mathrm{target}} \times (\mathrm{BW}/3)}{{r_{u,i}}^{-\alpha} 10^{-\eta_{u,i}/10}}\right) {d_{u,i}}^{-\alpha} 10^{-\xi_{u,i}/10}, & \text{cell edge,} \end{cases} \end{aligned} \tag{15b}$$

where $r_{u,i}$ represents normalized distance between the uth user and its corresponding BS in the ith cochannel cell.

3.2. System Capacity Analysis. Capacity is the highest rate at which information can be sent over the channel with

arbitrarily small probability of error [11] and the relation between capacity (bps/Hz) and signal-to-noise-plus-interference ratio (SINR) is given by

$$C = \left(1 + \log_2 \text{SINR}\right). \tag{16}$$

In cellular system, carrier frequency/frequencies will be reused by neighboring cells. Taking FRF into consideration, cellular capacity in bps/Hz/BS is given by

$$\overline{C} = \frac{1}{\text{FRF}}\left(1 + \log_2 \text{SINR}\right). \tag{17}$$

In hybrid FRF cellular system, since FRF 1 and FRF 3 are both used within a cell, cellular capacity depends on user's location and (17) is rewritten as

$$\overline{C} = \begin{cases} \log_2(1 + \text{SINR}), & \text{FRF1 area,} \\ \dfrac{1}{3}\log_2(1 + \text{SINR}), & \text{FRF3 area.} \end{cases} \tag{18}$$

In order to evaluate the cellular capacity, we are going to derive SINR in the next. For FDAAA, the signal power of array output can be calculated by

$$\begin{aligned} P_{\text{FDAAA}} &= E\left\{\frac{1}{N_c}\sum_{k=0}^{N_c-1}\hat{R}(k)\hat{R}^*(k)\right\} \\ &= \frac{1}{N_c}\sum_{k=0}^{N_c-1}\mathbf{W}_{\text{FDAAA}}{}^H(k)[\mathbf{R}_s(k) + \mathbf{R}_{NI}(k)] \\ &\quad \times \mathbf{W}_{\text{FDAAA}}(k), \end{aligned} \tag{19}$$

where $\mathbf{R}_s(k)$ is the autocorrelation matrix of the receive signal from the desired user, and $\mathbf{R}_{NI}(k)$ is the autocorrelation matrix of the receive signal from interfering users plus noise. Therefore, SINR can be obtained by

$$\begin{aligned} \text{SINR} &= \frac{\text{power of received signal}}{\text{power of interference + noise power}} \\ &= \frac{\sum_{k=0}^{N_c-1}\mathbf{W}_{\text{FDAAA}}(k)\mathbf{R}_s(k)\mathbf{W}_{\text{FDAAA}}(k)}{\sum_{k=0}^{N_c-1}\mathbf{W}_{\text{FDAAA}}{}^H(k)\mathbf{R}_{NI}(k)\mathbf{W}_{\text{FDAAA}}(k)}. \end{aligned} \tag{20}$$

Note that interference power also depends on the users' location and two cases should be considered:

Case 1 (Desired user is inside FRF 1 area). MUI power is given by

$$P_{\text{MUI},u} = \begin{cases} (E_s)_{\text{target}} \times \text{BW}, & \text{cell center,} \\ (E_s)_{\text{target}} \times \dfrac{\text{BW}}{3}, & \text{cell edge,} \end{cases} \tag{21}$$

and CCI power is given by

$$\begin{aligned} &P_{\text{CCI},u} \\ &= \begin{cases} \left(\dfrac{(E_s)_{\text{target}} \times \text{BW}}{r_{u,i}{}^{-\alpha}10^{-\eta_{u,i}/10}}\right) d_{u,i}{}^{-\alpha}10^{-\xi_{u,i}/10}, & \text{cell center,} \\ \left(\dfrac{(E_s)_{\text{target}} \times (\text{BW}/3)}{r_{u,i}{}^{-\alpha}10^{-\eta_{u,i}/10}}\right) d_{u,i}{}^{-\alpha}10^{-\xi_{u,i}/10}, & \text{cell edge.} \end{cases} \end{aligned} \tag{22}$$

Case 2 (Desired user is inside FRF 3 area). MUI power is given by

$$P_{\text{MUI},u} = \begin{cases} (E_s)_{\text{target}} \times \dfrac{\text{BW}}{3}, & \text{cell center,} \\ (E_s)_{\text{target}} \times \dfrac{\text{BW}}{3}, & \text{cell edge,} \end{cases} \tag{23}$$

and CCI power is given by

$$\begin{aligned} &P_{\text{CCI},u} \\ &= \begin{cases} \left(\dfrac{(E_s)_{\text{target}} \times (\text{BW}/3)}{r_{u,i}{}^{-\alpha}10^{-\eta_{u,i}/10}}\right) d_{u,i}{}^{-\alpha}10^{-\xi_{u,i}/10}, & \text{cell center} \\ \left(\dfrac{(E_s)_{\text{target}} \times (\text{BW}/3)}{r_{u,i}{}^{-\alpha}10^{-\eta_{u,i}/10}}\right) d_{u,i}{}^{-\alpha}10^{-\xi_{u,i}/10}, & \text{cell edge.} \end{cases} \end{aligned} \tag{24}$$

4. Impact of Antenna Placement

FDAAA receiver was proposed as a solution to combat MAI in frequency selective fading environment. In our previous study, it has been proved that when the antennas are considered to be uncorrelated with each other, FDAAA receiver has the ability to accommodate up to N_r users in a single cell and even in cellular environment when the FRF is big enough. However, the noncorrelation assumption is impractical and correlation often occurs and depends on the antenna placement in an array. To understand the impact of antenna placement, two parameters, antenna separation d and AOA spread Δ, are considered in this study. Equation (6) can be rewritten by

$$\mathbf{h}_{u,l} = h_{u,l}\mathbf{w}(\theta_{u,l}), \tag{25}$$

where $\mathbf{w}(\theta_{u,l})$ is the steering vector of the linear array, given by

$$\begin{aligned} \mathbf{w}(\theta_{u,l}) &= [w_0(\theta_{u,l}), w_1(\theta_{u,l}), \ldots, w_{N_r-1}(\theta_{u,l})]^T \\ &= \left[\exp\left(-j2\pi\frac{(0.5N_r - 0.5)}{\lambda}d\cos\,\theta_{u,l}\right),\right. \\ &\qquad \exp\left(-j2\pi\frac{(0.5N_r - 1.5)}{\lambda}d\cos\,\theta_{u,l}\right), \ldots, \\ &\qquad \left.\exp\left(j2\pi\frac{(0.5N_r - 0.5)}{\lambda}d\cos\,\theta_{u,l}\right)\right]^T. \end{aligned} \tag{26}$$

$\theta_{u,l}$ is uniformly distributed within a range of Δ and the probability density function of $\theta_{u,l}$ is given by

$$f(\theta_{u,l}) = \begin{cases} \dfrac{1}{\Delta}; & -\dfrac{\Delta}{2} + \theta_0 \le \theta_{u,l} \le \dfrac{\Delta}{2} + \theta_0, \\ 0; & \text{otherwise.} \end{cases} \tag{27}$$

The spatial correlation between the mth and nth antenna elements can be calculated by [12–15]:

$$\begin{aligned} D_s(m,n) &= \int_{\theta_{u,l}} w_m(\theta_{u,l})\, w_n^*(\theta_{u,l})\, f(\theta_{u,l})\, d\theta_{u,l} \\ &= \frac{1}{\Delta}\int_{-(\Delta/2)+\theta_0}^{(\Delta/2)+\theta_0} \exp\left(j2\pi\frac{m-n}{\lambda}d\cos\,\theta_{u,l}\right) d\theta_{u,l}. \end{aligned} \tag{28}$$

Table 1: Simulation parameters.

Transmitter	Data modulation	QPSK
	FFT size	$N_c = 256$
	TPC	Slow TPC
	Number of user per cell	$U = 1 \sim 8$
	No. of CCI cells	$I = 18$
	Target receive E_s/N_0 per antenna	10 dB
Channel	Channel model	Frequency-selective block Rayleigh fading
	Power delay profile	$L = 16$ uniform power delay
	Angle spread of resolvable paths (AOA)	$\Delta = 30°, 60°, 180°, 360°$
	Path loss exponent	$\alpha = 3.5$
	Standard deviation of shadowing losses	$\xi = 6$ dB
	Channel State Information	Available only for user within the desired cell
	Nominal angle	Random
Receiver	No. of antennas	$N_r = 8$
	Antenna separation	$\lambda/2, \lambda, 5\lambda, 10\lambda$
	Channel estimation	Ideal

According to (28), the correlation between antenna elements as a function of AOA spread Δ as well as antenna separation d is calculated. The antenna correlation for $\theta_0 = 60°$ is shown in Figure 5. It is shown that when d increases, the antenna correlation decreases with vibration and finally converges to zero when d becomes infinite. In the extreme case when $d = 0$, all the antenna elements in the array become completely correlated. On the other hand, to increase the AOA spread Δ will speed up the convergence to zero. Therefore, in order to have less correlation between antennas, two possible ways are to increase d by occupying more space or to increase Δ by introducing more reflectors around the antenna array.

In addition, the antenna correlation will also be affected by angle θ_0 and the relation between antenna correlation and θ_0 is shown in Figure 6 where $d = \lambda/2$ is used. It is shown that the antenna correlation has the smallest value when $\theta_0 = 90°$ or $\theta_0 = 270°$. In other words, in order to reduce the antenna correlation, the third way is to adjust the array plane to be vertical to the incoming waveform.

5. Numerical Result

In the next, we are going to study the impact of antenna placement on the uplink cellular capacity using FDAAA receiver following (18) by Monte Carlo simulations. The parameters to be used are listed in Table 1.

In order to calculate the capacity for hybrid FRF cellular system, the hybrid FRF scheme, that is, FRF 1 area and FRF 3 area allocation within each cell should be determined at the first place. The cellular capacity will then be calculated based on the hybrid FRF scheme. In order to optimize the capacity performance, hybrid FRF is determined as

$$\text{FRF}_{\text{hybrid}} = \arg\min_{\text{FRF}=\{1,3\}} \frac{1}{\text{FRF}} \left(1 + \log_2 \text{SINR}\right). \quad (29)$$

For example, when antenna separation is $d = \lambda/2$ and AOA spread $\Delta = 360°$, hybrid FRF scheme with varying number of users is shown in Figure 7 where the FRF 1 area and FRF 3 area are separated by the colored circular curves. It is natural to observe that the FRF 1 area decreases when the number of users in each cell increases in order to optimize the cellular capacity when CCI power increased.

In the next, impact of antenna placement on the cellular capacity will be studied and our focus is on cellular outage

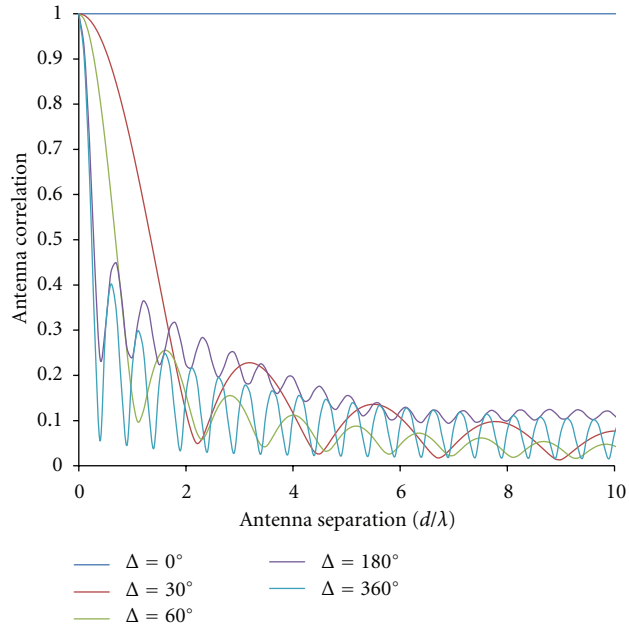

Figure 5: Antenna correlation for $\theta_0 = 60°$.

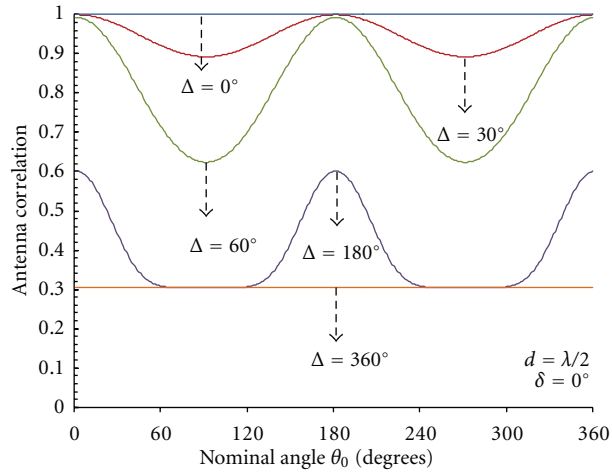

Figure 6: Relation between antenna correlation and θ_0.

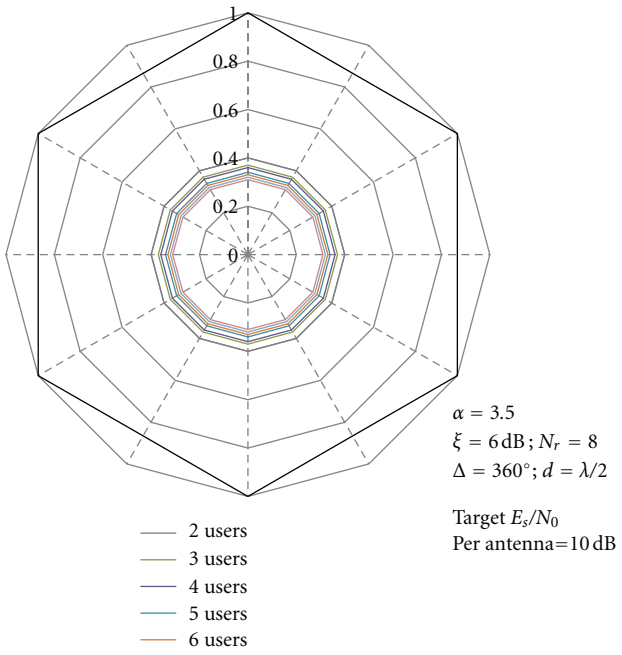

Figure 7: Hybrid FRF scheme with varying number of users.

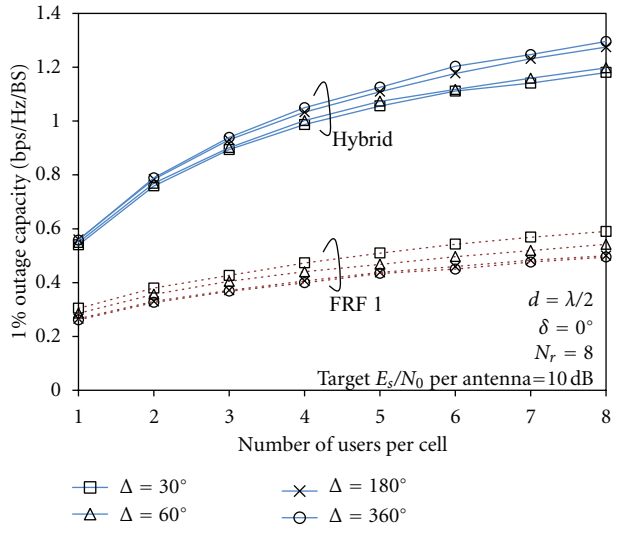

Figure 8: Cellular outage capacity with 1% outage probability.

capacity (the value that cellular capacity falls below with the outage probability) [16]. At first, the impact of AOA spread on cellular outage capacity is considered. In order to observe the effect of hybrid FRF algorithm, cellular capacity of single frequency reuse (FRF = 1) system is also calculated to make a comparison. The simulation results of 1% and 10% outage capacity are shown in Figures 8 and 9, respectively. It can be observed that the when AOA spread Δ increases from 30° to 360°, the cellular capacity increases for both hybrid FRF and FRF 1 cases. Recall that in Figure 5, we observed decreased antenna correlation when Δ increases. Actually, when $d = \lambda/2$ is used, FDAAA uses the correlation between

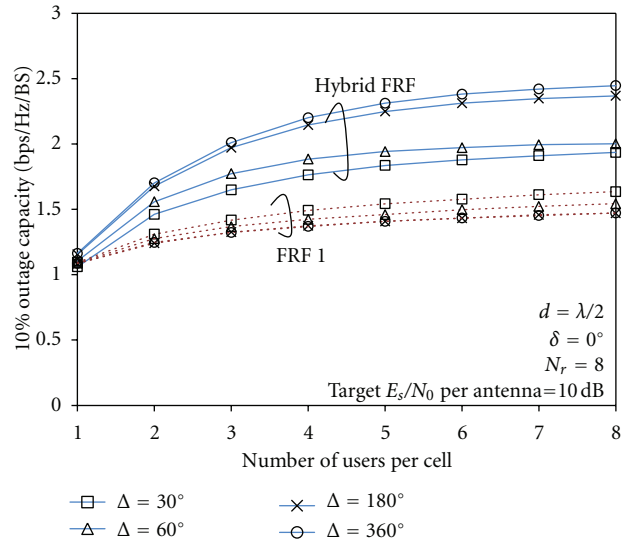

Figure 9: Cellular outage capacity with 10% outage probability.

antennas to generate beams in the directions of desired user and nulls in the directions of interfering users. When antenna correlation increases, the radiation pattern of the array will not be good enough and nonzero array gain will occur in the should-be-null directions, as shown in Figure 10. However, it is also observed that the capacity increase by increasing the AOA spread is quite limited, and the residue MAI should be the limiting factor.

The impact of antenna separation d is considered in the following. Assuming AOA spread $\Delta = 30°$, the cellular outage capacity is calculated for $d = \lambda/2$, $d = \lambda$, $d = 5\lambda$ and 10λ. The results corresponding to 1% and 10% outage probability are shown in Figures 11 and 12, respectively. It is observed that the cellular capacity can be obviously increased when the antenna separation increases. Recall that in Figure 5 we observed decreased antenna correlation when d increases and when d becomes larger than 5λ, antenna correlation drops to below 0.1, and the antenna elements can be treated as independent. In this situation, no beams or nulls will be generated (as shown in Figure 13) and diversity gain of multiple antennas can be utilized to combat MAI, and therefore maximize the achievable SINR.

In addition, it can be observed from Figures 8-9 and Figures 11-12 that the cellular outage capacity can be increased by using hybrid FRF and the increase in percentage is summarized in Tables 2 and 3 for $d = \lambda/2$ and $\Delta = 30°$, respectively. It is now obvious that by using hybrid FRF, cellular outage capacity, especially when the outage probability is low, can be greatly increased by using hybrid FRF. As we know that outage capacity is usually contributed by the users near the cell edge and the quality of service (Qos) of these users always suffers from strong CCI. Therefore, hybrid FRF together with FDAAA receiver is an effective solution to improve the Qos of the cell edge users and therefore can help to improve the fairness among users as well.

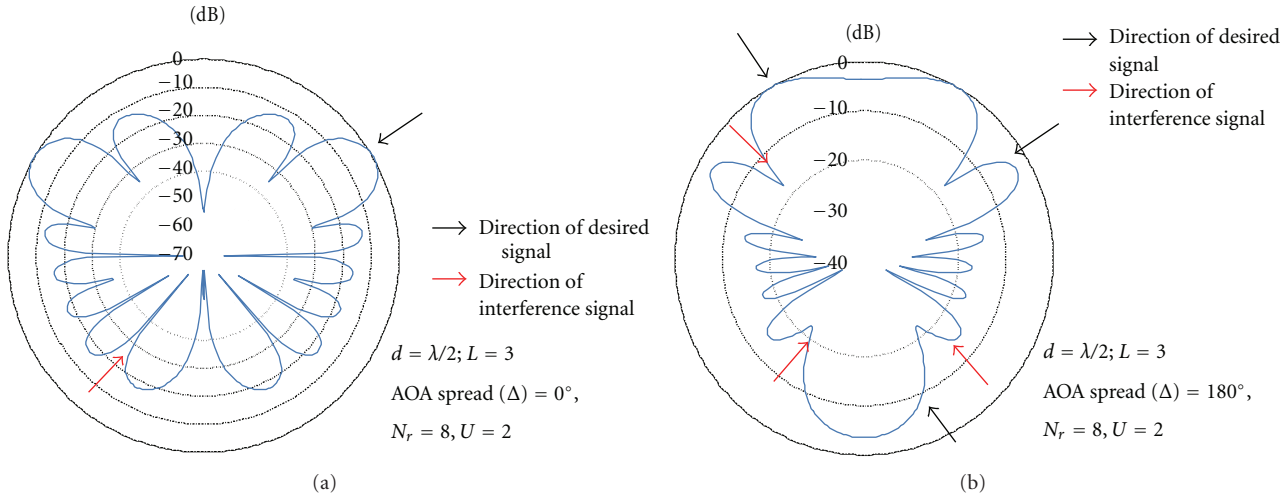

Figure 10: FDAAA Radiation pattern change from $\Delta = 0°$ to $\Delta = 180°$ where nonzero array gain appears in should-be-null direction.

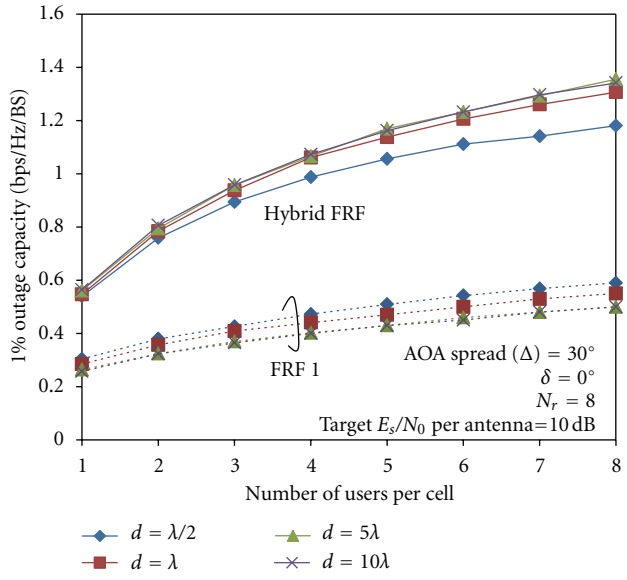

Figure 11: Cellular outage capacity with 1% outage probability.

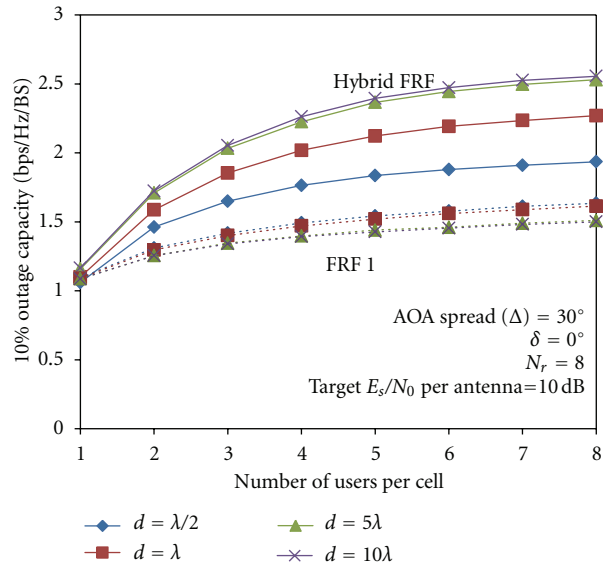

Figure 12: Cellular outage capacity with outage probability of 10%.

Table 2: Cellular capacity increase by using hybrid FRF ($d = \lambda/2$).

Outage probability	Capacity increase			
	$\Delta = 30°$	$\Delta = 60°$	$\Delta = 180°$	$\Delta = 360°$
1%	110%	129%	156%	168%
10%	19%	33%	61%	67%

Table 3: Cellular capacity increase by using hybrid FRF ($\Delta = 30°$).

Outage probability	Capacity increase			
	$d = \lambda/2$	$d = \lambda$	$d = 5\lambda$	$d = 10\lambda$
1%	110%	142%	172%	174%
10%	19%	41%	68%	71%

6. Conclusions

In this paper, the impact of antenna placement on the FDAAA receiver in hybrid FRF cellular system has been studied. Two parameters, antenna separation and AOA spread, have been considered. Taking the hybrid FRF into consideration, cellular capacity is derived and the impact of antenna placement on cellular capacity is then evaluated. It has been shown that increasing the AOA spread can reduce the antenna correlation, and therefore can increase the cellular capacity by using FDAAA receiver. On the other hand, increasing the antenna separation to above 5λ will reduce the antenna correlation to almost zero and can greatly increase the cellular capacity. In addition, the comparison between hybrid FRF and FRF 1 has shown that hybrid FRF algorithm can effectively improve the cellular outage

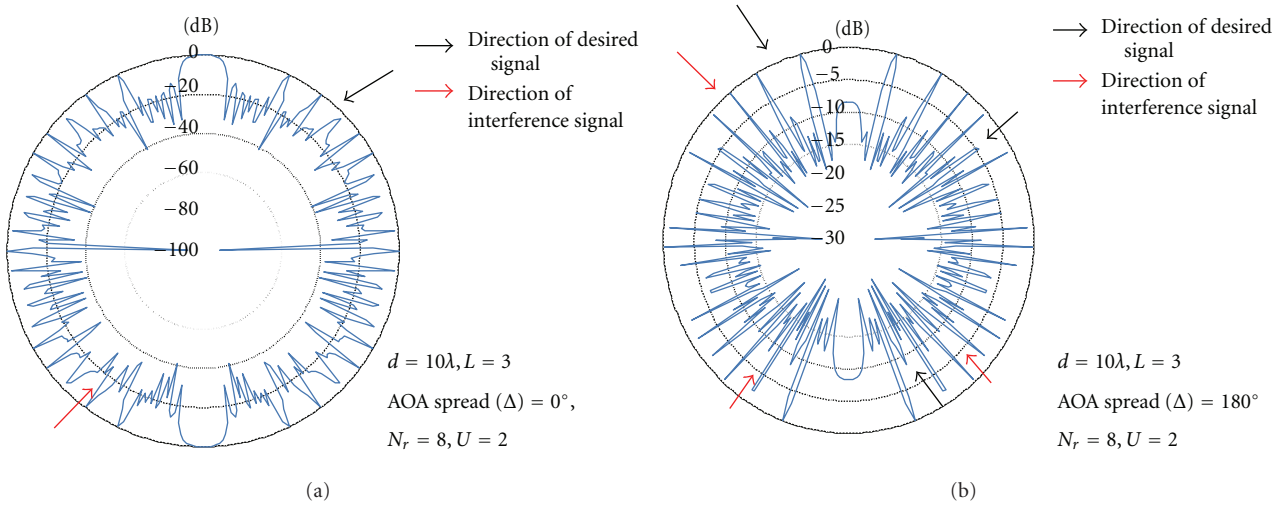

Figure 13: FDAAA radiation pattern when antenna separation $d = 10\lambda$.

capacity, and therefore hybrid FRF together with FDAAA receiver is a good solution for uplink transmission in cellular system.

Acknowledgment

This work was supported in part by 2011 KDDI Research Grant Program (J110000208).

References

[1] H. G. Myung, J. Lim, and D. J. Goodman, "Single carrier FDMA for uplink wireless transmission," *IEEE Vehicular Technology Magazine*, vol. 1, no. 3, pp. 30–38, 2006.

[2] S. Jimaa, K. K. Chai, Y. Chen, and Y. Alfadhl, "LTE-A an overview and future research areas," in *Proceedings of the IEEE 7th International Conference on Wireless and Mobile Computing, Networking and Communications (WiMob)*, pp. 395–399, Wuhan, China, October 2011.

[3] F. Adachi, H. Tomeba, and K. Takeda, "Frequency-domain equalization for broadband single-carrier multiple access," *IEICE Transactions on Communications*, vol. 92, no. 5, pp. 1441–1456, 2009.

[4] J. H. Winters, "Signal acquisition and tracking with adaptive arrays in the digital mobile radio system IS-54 with flat fading," *IEEE Transactions on Vehicular Technology*, vol. 42, no. 4, pp. 377–384, 1993.

[5] W. Peng and F. Adachi, "Frequency domain adaptive antenna array algorithm for single-carrier uplink transmission," in *Proceedings of the IEEE 20th Personal, Indoor and Mobile Radio Communications Symposium (PIMRC' 09)*, pp. 2514–2518, Tokyo, Japan, September 2009.

[6] B. Kang, O. Nakamura, H. Tomeba, and F. Adachi, "Performance comparison of Pre-FFT and Post-FFT OFDM adaptive antenna array," in *Proceedings of the 3rd IEEE VTS Asia Pacific Wireless Communications Symposium*, Daejeon, South Korea, August 2006.

[7] K. Takeda, R. Kawauchi, and F. Adachi, " Single-carrier uplink transmission using frequency-domain equalization," in *Proceedings of the 9th Symposium on Wireless Personal Multimedia Communications*, pp. 776–780, Hyatt Regency La Jolla, San Diego, Calif, USA, September 2006.

[8] W. Peng and F. Adachi, "Multi-user hybrid FRF algorithm for downlink cellular MIMO systems," in *Proceedings of the IEEE 20th Personal, Indoor and Mobile Radio Communications Symposium (PIMRC' 09)*, pp. 968–972, Tokyo, Japan, September 2009.

[9] W. Peng and F. Adachi, "Frequency domain adaptive antenna array for broadband single-carrier uplink transmission," *IEICE Transactions on Communications*, vol. 94, no. 7, pp. 2003–2012, 2011.

[10] J. C. Liberti and J. S. Rappaport, *Smart Antenna for Wireless Communication: IS-95 and Third Generation CDMA Applications*, Prentice Hall, Upper Saddle River, NJ, USA, 1995.

[11] J. G. Proakis, *Digital Communications*, McGraw Hill, New York, NY, USA, 2001.

[12] J. Salz and J. H. Winters, "Effect of fading correlation on adaptive arrays in digital mobile radio," *IEEE Transactions on Vehicular Technology*, vol. 43, no. 4, pp. 1049–1057, 1994.

[13] K. Watanabe, S. Sampei, and N. Morinaga, "Effect of angle spread on system capacity in DS/CDMA cellular system using adaptive array antenna," in *Proceedings of the 11th IEEE International Symposium on Personal, Indoor and Mobile Radio Communications (PIMRC' 00)*, vol. 1, pp. 98–102, September 2000.

[14] J. A. Tsai, R. M. Buehrer, and B. D. Woerner, "The impact of AOA energy distribution on the spatial fading correlation of linear antenna array," in *Proceedings of the IEEE Vehicular Technology Conference (VTC' 02)*, pp. 933–937, May 2002.

[15] F. Adachi, M. T. Feeney, A. G. Williamson, and J. D. Parsons, "Cross-correlation between the envelopes of 900 MHz signals received at a mobile radio base station site," *IEE Proceedings*, vol. 133, no. 6, pp. 506–512, 1986.

[16] K. Adachi, F. Adachi, and M. Nakagawa, "On cellular MIMO spectrum efficiency," in *Proceedings of the 66th IEEE Vehicular Technology Conference (VTC-Fall'07)*, pp. 417–421, Baltimore, Md, USA, October 2007.